AIP | Applied Physics Letters

Ellipsometric investigation of nitrogen doped diamond thin films grown in microwave CH4/H2/N2 plasma enhanced chemical vapor deposition

Mateusz Ficek, Kamatchi J. Sankaran, Jacek Ryl, Robert Bogdanowicz, I-Nan Lin, Ken Haenen, and Kazimierz Darowicki

Citation: Applied Physics Letters **108**, 241906 (2016); doi: 10.1063/1.4953779
View online: http://dx.doi.org/10.1063/1.4953779
View Table of Contents: http://scitation.aip.org/content/aip/journal/apl/108/24?ver=pdfcov
Published by the AIP Publishing

Ellipsometric investigation of nitrogen doped diamond thin films grown in microwave $CH_4/H_2/N_2$ plasma enhanced chemical vapor deposition

Mateusz Ficek,[1,2,a] Kamatchi J. Sankaran,[2,3] Jacek Ryl,[4] Robert Bogdanowicz,[1,5] I-Nan Lin,[6] Ken Haenen,[2,3] and Kazimierz Darowicki[4]
[1]*Department of Metrology and Optoelectronics, Faculty of Electronics, Telecommunications and Informatics, Gdansk University of Technology, 11/12 G. Narutowicza St., 80-233 Gdansk, Poland*
[2]*Institute for Materials Research (IMO), Hasselt University, Wetenschapspark 1, B-3590 Diepenbeek, Belgium*
[3]*IMOMEC, IMEC vzw, Wetenschapspark 1, B-3590 Diepenbeek, Belgium*
[4]*Department of Electrochemistry, Corrosion and Material Engineering, Gdansk University of Technology, 11/12 Narutowicza St., 80-233 Gdansk, Poland*
[5]*Materials and Process Simulation Center, California Institute of Technology, Pasadena, California 91125, USA*
[6]*Department of Physics, Tamkang University, Tamsui 251, Taiwan*

(Received 29 February 2016; accepted 31 May 2016; published online 14 June 2016)

The influence of N_2 concentration (1%–8%) in $CH_4/H_2/N_2$ plasma on structure and optical properties of nitrogen doped diamond (NDD) films was investigated. Thickness, roughness, and optical properties of the NDD films in the VIS–NIR range were investigated on the silicon substrates using spectroscopic ellipsometry. The samples exhibited relatively high refractive index (2.6 ± 0.25 at 550 nm) and extinction coefficient (0.05 ± 0.02 at 550 nm) with a transmittance of 60%. The optical investigation was supported by the molecular and atomic data delivered by Raman studies, bright field transmission electron microscopy imaging, and X-ray photoelectron spectroscopy diagnostics. Those results revealed that while the films grown in CH_4/H_2 plasma contained micron-sized diamond grains, the films grown using $CH_4/H_2/(4\%)N_2$ plasma exhibited ultrananno-sized diamond grains along with *n-diamond* and *i-carbon* clusters, which were surrounded by amorphous carbon grain boundaries. *Published by AIP Publishing*. [http://dx.doi.org/10.1063/1.4953779]

Polycrystalline diamond films deposited by chemical vapor deposition (CVD) are excellent materials for microelectronic devices including high-power switches, high-power and high-speed amplifiers, and integrated circuits.[1] Furthermore, the diamond has excellent chemical and mechanical properties, such as high thermal conductivity, high radiation resistance, high chemical stability, and wide electronic band gap, and dopant-controlled electrical conductivity from highly insulating to near metallic, depending on the chosen dopant.[2–5] Growth of polycrystalline diamond films is usually by CVD using different gas mixtures and reactor systems. The addition of p-type (e.g., boron) or n-type (e.g., phosphorus, sulphur, etc.) dopants can render microcrystalline diamond conductive. Diverse reports on B-, P-, and S-doped diamond highlight the effect of various film deposition conditions and structural evolution, which facilitates in defining the properties of the films.[6–8] Nitrogen is another potential n-type dopant in diamond since it incorporates either diluted in substitutional sites of the diamond lattice (type Ib—low percentage of N) or in small aggregates (type Ia—high percentage of N). Nitrogen incorporation results in significant mechanical stress and increases the number of vacancy defects due to distortion of the diamond lattice.[9–11] Several articles were published on the influence of nitrogen on the growth rate and quality of diamond films.[10–14] These[15] experiments were done using gas mixtures of $CH_4/H_2/N_2$ in microwave plasma reactors.

Most studies concern the nitrogen-doped diamond (NDD)-like carbon or carbon films deposited by RF plasma[12] or filtered cathodic vacuum arc (FCVA) technique.[16] Both RF plasma and FCVA techniques enable us to grow conductive N-doped carbon films (resistivity of ca. tens of Ω cm) with a refractive index $n > 2$. Nevertheless, those films exhibit amorphous structure with high amount of sp^2 phases, which impairs optical transmittance due to high k value[17] or electrochemical performance (e.g., organic matter adsorption and electrode fouling).[18] Microwave plasma enhanced CVD (MW PECVD) process results in polycrystalline nitrogen-doped diamond (NDD) films with high sp^3 content possessing low electrical conductivity and superior field emission properties.[9]

In majority, the previous investigations have been focused on the use of surface morphology, microstructure, and bonding structure modified due to the addition of nitrogen species into the CH_4/H_2 plasma. Nevertheless, the conductive NDD films attracting great interest in the field of optical applications including energy conversion[19] or biosensing.[3] To address these issues, we present the optical performance of NDD films in function of wide range of nitrogen addition in the microwave plasma phase. Moreover, we reference the obtained optical properties to the structural and atomic composition of NDD films.

Thus, in this contribution, we investigate the NDD films grown on a n-type mirror polished Si wafers in MWPECVD (2.45 GHz; 600 IPLAS-CYRANNUS-I, Troisdorf, Germany) system. The details of the growth is reported elsewhere.[9] Mixtures of CH_4, H_2, and N_2 were used as the reactant gases for the microwave discharges. The grown samples were designated as "NDD_z" films, where z is the percentage concentration of N_2 in a gas phase varying from 0 to 10 sccm (0% to 8% of total). The growth results in the low surface resistivity

[a]Author to whom correspondence should be addressed. Electronic mail: rbogdan@eti.pg.gda.pl. Telephone: +48 58 347 2482. Fax: +48 58 347 18 48

of NDD samples in the range from 7×10^4 to 30 Ω cm, from 1% to 8% of nitrogen concentration, respectively.

Fig. 1(a) displays the UV-Raman spectroscopy ($\lambda = 325$ nm) (Lab Raman HR800, Jobin Yvon, France) of the different N_2 concentrations of samples. The deconvolution of Raman spectra using Lorentz curves (see Fig. S1—supplementary material)[20] reveals that besides the G-band (1569–1578 cm^{-1}) [sp^2-hybridized carbon [graphite or amorphous carbon (*a-C*)] and the diamond Raman signal [sp^3-diamond—1334 cm^{-1}], the spectrum shown in Fig. 1(a) for the NDD films displays a wide D-band in the range of 1379–1382 cm^{-1}[disorder-induced peak]. The sp^3/sp^2 band ratio of diamond peak and G-band gradually decreases due to nitrogen incorporation causing tetrahedral structure deformation (see the inset in Fig. 1(a)).[21,22] Graph of I(D)/I(G) ratios with corresponding D-band and G-band positions is plotted in the supplementary material—Figs. S2(a) and S2(b).[20]

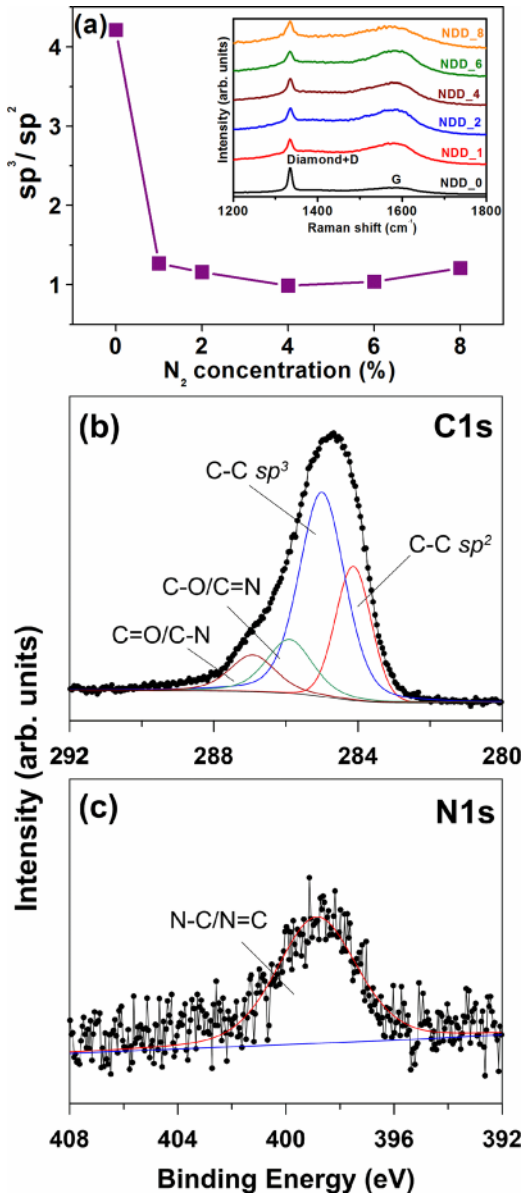

FIG. 1. The (a) UV-Raman spectroscopy and the sp^3/sp^2 ratio of diamond films grown using different N_2 concentrations (0%–8%) in CH_4/H_2 plasma (inset: Raman spectra of NDD films). The (b) C1s and (c) N1s XPS spectra of the synthesized NDD films with 4% of N_2 concentration in the plasma.

The X-ray photoelectron spectroscopy (XPS) investigation was carried out using Escalab 250Xi (ThermoFisher Scientific, United Kingdom) utilizing monochromatic Al Kα source gun and a spot diameter of 650 μm with charge neutralization implemented by means of a flood gun [see Figs. 1(b) and 1(c)]. High-resolution spectra used during deconvolution were recorded at a pass energy 10 eV and energy step size of 0.1 eV. In order to normalize spectroscopic measurements, binding energy (BE) was calibrated for peak characteristics of neutral carbon 1 s (BE = 284.6 eV). Data analysis was performed using Avantage v.5 software.

Deconvolution of XPS spectra was carried out using earlier studies on similar electrodes.[23] C1s spectra contained four peaks (see Fig. 1(b), Table I, and Fig. S3 in the supplementary material)[20] and two peaks located at binding energies of ~284.2 and ~285.0 eV contributed to sp^2 C-C and sp^3 C-C bond atoms, respectively.[24] The peaks at 285.8 eV corresponds to sp^2 C = N but may as well be interpreted as C-O bonds due to small energy difference between those peaks. Similar case applies for sp^3 C-N which was collectively deconvoluted together with carbonyl, carboxyl as well as ether bonds using peak located at ~287.1 eV. The N1s XPS spectrum (NDD_4) with peak at 399 eV is illustrated in Fig. 1(c). The amount of analyzed O1s was equal up to even 15%, which results from the exposure of samples to the atmosphere and is in good agreement with previous XPS studies.[25] Moreover, the [C]/[N], [C]/[O], and [O]/[N] ratios are listed in Table S1 in the supplementary material[20] for direct comparison.

The bright field transmission electron microscopy (BF-TEM, Joel 2100 F, Japan) study was performed for deeper understanding the evolution of microstructure of the NDD films [Figs. 2(a)–2(d)]. Additionally, low resolution BF TEM images have been shown in the supplementary material (Fig. S4).[20] Micrographs of NDD films display polycrystalline structure consisting of neighbouring diamond grains. The BF-TEM images have been accompanied by the selective area electron diffraction (SAED) [insets, Figs. 2(a)–2(d)]. The SAEDs demonstrate that the low doped NDD films consist of randomly oriented diamond crystallites and just the grains oriented near the zone-axis strongly diffract electrons [SAED, inset Fig. 2(a)].

All the doping levels reveal in the SAED the commonly observed (111), (220), and (311) lattice planes, which correspond to the randomly oriented ultra-small diamond clusters, coexisting with discrete diffraction spots, which represent

TABLE I. Percentage contribution of the C1s, N1s, and O1s peaks in the NDD films estimated by XPS.

Element+ BE (eV) / %N	C1s				N1s	O1s
	sp^2C-C	sp^3C-C	C-O/C = N	C = O/C-N		
	284.2	285.0	286.1	287.1	398.9	531.7
NDD_0	20.0	41.8	12.7	7.1	2.6	15.9
NDD_1	19.3	43.5	16.3	9.4	3.1	8.4
NDD_2	31.5	33.2	16.8	5.2	2.8	10.5
NDD_4	19.5	41.8	11.5	7.8	3.1	16.3
NDD_6	16.2	46.4	11.4	6.0	3.6	17.9
NDD_8	40.5	31.0	6.4	2.7	1.6	17.8

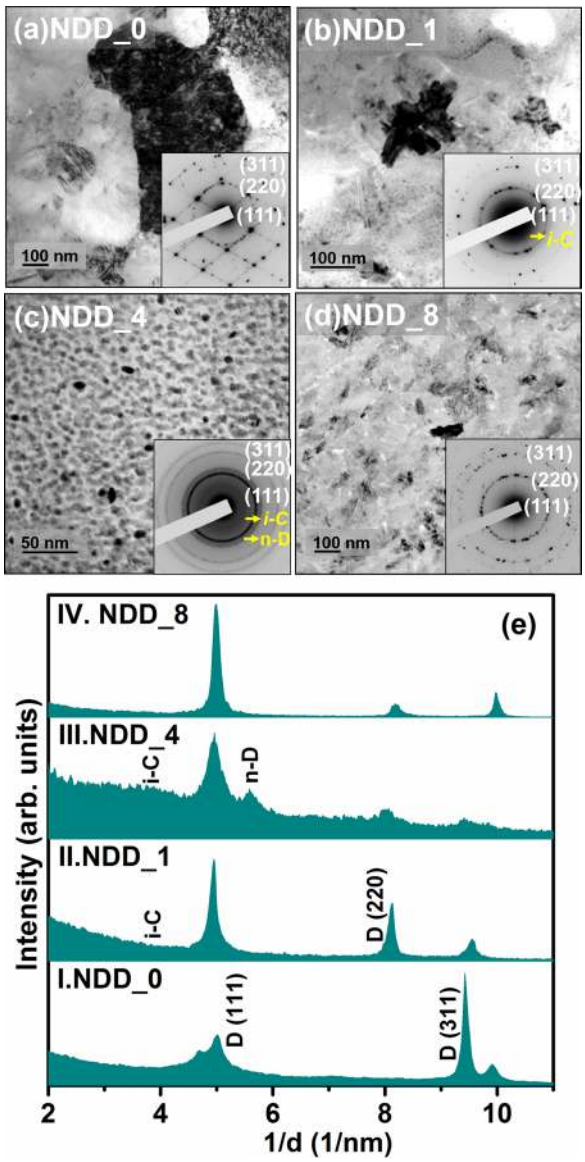

FIG. 2. The (a)–(d) BF-TEM images of NDD films grown using 0%, 1%, 4%, and 8% N_2 in CH_4/H_2 plasma (insets: SAED patterns) and (e) corresponding linear diffraction patterns (LDP).

large diamond grains. Since the N_2 increases in the plasma, the crystalline structure of the diamond films is gradually transformed to nano-sized (avg. diameter of approx. 5 nm), which are to randomly oriented, spherical particulates with uniform size distribution [Fig. 2(c)]. Furthermore, the diffraction ring of smaller size than the $(111)_D$ ring is attributed to *i-carbon* (*i-C*), the bcc structured carbon with $a_0 = 0.432$ nm,[26,27] while the larger one corresponds to (200) of *n-diamond* (*n-D*) phase, the fcc structured carbon with cell parameter $a_0 = 0.356$ nm.[26,28] The highest nitrogen doping (8% of N_2 in the plasma) initiate the formation of elongated agglomerates of grains of a few hundred nanometers in size. The SAED of NDD_8 shows [inset, Fig. 2(d)] spotty rings inferring the formation of the large diamond aggregates with randomly oriented diamond grains in the film. Unlike those observed for the low doped films, no additional diffraction rings besides the main (111), (220), and (311) diamond ones are visible for the NDD_8 films. Thus, the *i-C* and *n-D* phases are minor in those samples. As can be seen in the SAED in Fig. 2(d), the central diffused ring is also less pronounced here indicating the smaller existence of graphitic (or *a-C* phase) in these films when compared with low doped (i.e., NDD_1 and NDD_4).

The microstructural evolution of NDD films is best illustrated by the LDP, which are derived from the SAED, shown in Figs. 2(a)–2(d), and are revealed in Fig. 2(e). Spectrum I discloses that the CH_4/H_2 plasma grown diamond films comprise only diamond spectrum representing the uniformly large diamond grains granular structure for 0% N_2 films. The addition of small amount of N_2 (1%N_2) in CH_4/H_2 plasma directs to the induction of *i-C* phases (spectrum II), which acquaint as some ultra-small particulates in BF-TEM image [Fig. 2(b)]. The proportion of nano-sized particulates raised with the amount of N_2 added in the plasma, ensuing in a film containing uniformly nano-sized particulates of *n-D*, *i-C*, and nano-diamond in 4%N_2 samples [spectrum III and Fig. 2(c)]. Further increase in N_2-content changes the *n-D* and *i-C* particulates into aggregates of a few hundred nanometers diamond crystals [spectrum IV and Fig. 2(d)]. Moreover, the detailed investigations of NDD_8 were carried out from HRTEM and presented in the supplementary material (Fig. S5)[20] revealing the presence of graphitic or *a-C* phases in the NDD_8 sample [cf. Fig. 2(d)].

The optical parameters of NDD films were studied by a Jobin-Yvon UVISEL phase-modulated ellipsometer (HORIBA Jobin-Yvon, Inc., Edison, USA) in a wavelength range from 260 to 830 nm. The experiments were performed at room temperature and with the angle of incidence fixed at 70°. The ellipsometric fitting was based on a four-phase optical model (air/surface roughness film (SRL)/NDD/silicon). The dispersion of silicon wafer was taken from the database.[29] The dielectric function of the SRL was estimated using the Bruggeman effective medium approximation (EMA) of mixture of 50% NDD and 50% void. The NDD film was fitted to the Tauc–Lorentz oscillator (TL) model[30] and measured by mean-square minimization error (MSE).[31] The mean estimation error of n and k was less than <5% for the analysed samples.

Based on the outcome of spectroscopic ellipsometry (SE) analysis, the thickness and optical constants, including the refractive index $n(\lambda)$ and extinction coefficient $k(\lambda)$, were estimated [Figs. 3(a) and 3(b)]. While k gradually decreases with nitrogen concentration from 0.05 to values close to zero, n first jumps from 2.5 to almost 2.4 at low nitrogen concentration after which it regularly decreases with a further increase in the nitrogen concentration (values at 550 nm) [Fig. 3(a)]. Apart from the shift of the $n(E)$ level, the slight shift of n towards higher photon energy with the higher nitrogen dopant concentration was observed. Trend of $k(E)$ agrees with the refractive index indicating an enhancement in optical transparency [Fig. 3(c)].

The initial increment of the refractive index for 1% nitrogen concentration (NDD_1) could be explained by a decrease of sp^2 hybridized clusters in sp^3 hybridized matrix (increment of I(D)/I(G) ratio, Fig. S2—supplementary material)[20] or by a gradual change of film structure and density versus depth. Silicon wafer is a monocrystalline substrate inducing the formation of a dense carbon film with higher sp^3/sp^2 ratio near its surface comparing to the properties towards the top of the film. Thus, the NDD films with higher thickness are influenced by this phenomenon. Since the NDD_0 sample results

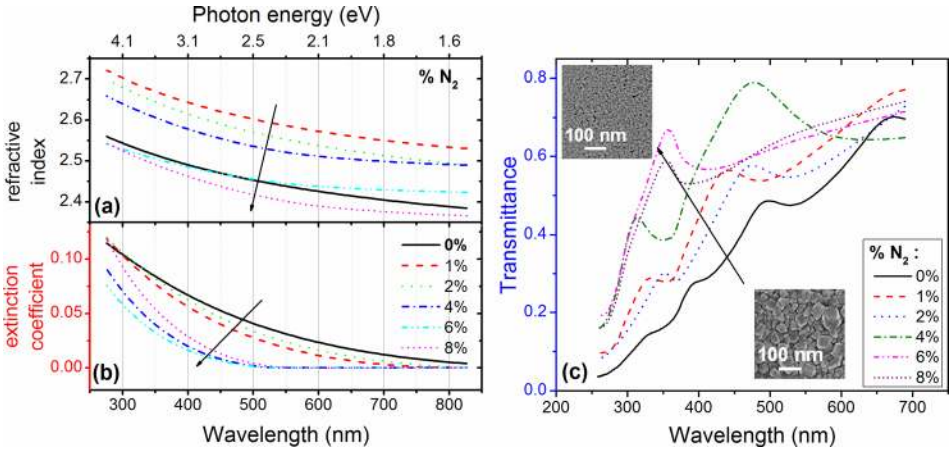

FIG. 3. Spectral dependence of refractive index *n* (a) and extinction coefficient *k* (b) of nitrogen-doped diamond films as a function of various admixture of N_2 in CH_4/H_2 plasma. Intrinsic optical transmittance (c) of NDD samples deposited at different nitrogen percentages. Inset: SEM micrographs diamond films surface using (bottom) 0% N_2 and 8% N_2 (top) concentrations in CH_4/H_2 plasma.

in 350 nm of thickness, while NDD_1 displays 210 nm. This phenomenon is not only supported by our previously reported cross-sectional SEM studies[9] but also was reported by others.[32] The further decrease of both n and k could be attributed to phases like *n-D, i-C,* or *a-C* for higher nitrogen concentrations as revealed by TEM studies (cf. Fig. 2). In comparison, Gharibyan *et al.*[33] reported refractive indices in the range 1.46–2.85 in the case of nitrogen concentration variation in the region 5%–90% for the PECVD grown nitrogen-doped diamond-like carbon (N:DLC) films.[33] Next, the FCVA deposition results in the N-doped diamond films with n in the range from 2.3 to 2.9 as communicated by Cheah *et al.*[16] In case of highly nitrogen doped films, both groups achieved *k* values close to zero for the phonon energy level below 3 eV.

Figures 3(c) and 4(a) illustrate the intrinsic transmittance of NDD samples doped with various concentrations of nitrogen. It could be noticed that doping of nitrogen results

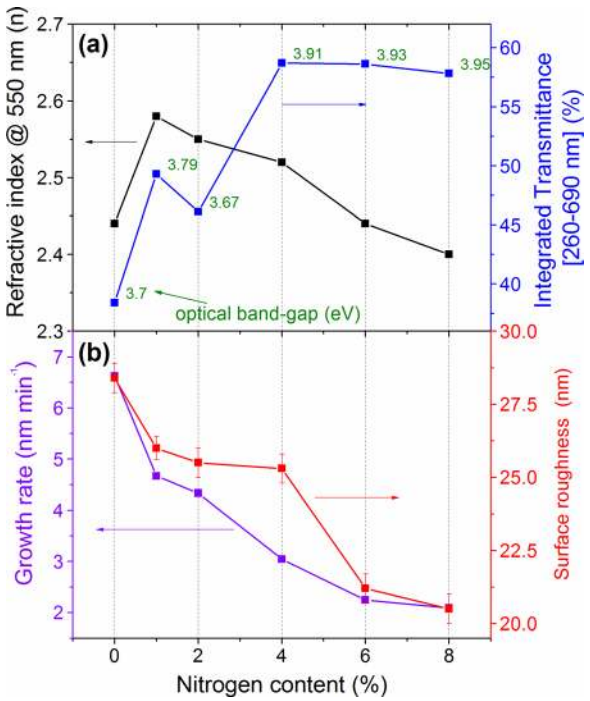

FIG. 4. The parameters of NDD films: (a) refractive index recorded at 550 nm and integrated transmittance at the wavelength range of 260–690 nm; (b) film growth rate and SRL as determined by spectroscopic ellipsometry vs various nitrogen contents in the gas phase. The values of the optical band-gap E_g are illustrated at the transmittance plot (a).

in the gradual increase of the optical transmittance up to the value of approx. 60%. This effect is attributed to the spherical nano-particulates as well to the lower thickness of highly doped samples, thereby limiting the influence of depth variation of the film structure.

Next, the values of growth rate and surface roughness (SRL) of NDD films deposited at different nitrogen concentrations are illustrated in Figure 4(b). It is noteworthy that the deposition time was kept at 60 min for all the investigated samples.

The NDD growth rate estimated by SE has been found to decrease noticeably on the addition of N_2 in the plasma [Fig. 4(b)]. These observations are in agreement with our previous findings.[9] Moreover, a similar trend was reported by Badzian *et al.*[11] or Bohr *et al.*[14] and attributed to CN radicals formed in $N_2/H_2/CH_2$ reducing the CH_3 concentration, thereby the diamond growth was inhibited.

As shown in Figure 4(a), the *Eg* jumps from approximately 3.7 to 3.9 eV as the nitrogen concentration changes from 2 at.% to 4 at.%. An opposite trend was reported by Hayashi *et al.*[13] for RF PECVD grown films, where the incorporated nitrogen leads to the broadening of the π and π^* bands and the disorder in the crystalline boundaries effects in a reduced energy gap generally due to band tailing. In our case, the N_2 incorporation is relatively smaller avoiding high disorder of boundaries; consequently, the effect *Eg* value is not comparable and needs to be further investigated.

Furthermore, it should be assumed that as the low admixtures of nitrogen provide compensation of the dangling bands in the *a-C* structure and increase the sp^3 fraction of the NDD film as reported by Silva *et al.*[10] or Cheah *et al.*,[16] while higher percentages of nitrogen in the gas phase generate nitrogen related centers causing tetrahedral structure distortion.[34]

Since *n* is correlated with the sp^3 content and material's density,[35] the results suggest that the higher refractive index [Fig. 4(a)] is the synergistic effect of sp^3 hybridisation (*3C*-diamond) and *n-D*, *i-C* phases. Higher content of sp^3 phase results in the higher activation energy shifting the Fermi level towards the conduction band, thereby optical band-gap increases.

In summary, the influence of nitrogen doping level on the polycrystalline CVD grown NDD films was particularly studied. The samples exhibited relatively high refractive index (2.6 ± 0.25 at 550 nm) and extinction coefficient (0.05 ± 0.02 at 550 nm) for low nitrogen doping level and these decrease

with the wavelength. Microstructural results revealed that while the films grown in CH_4/H_2 plasma contained micron-sized diamond grains, the films grown using $CH_4/H_2/(4\%)N_2$ plasma exhibited ultrananno-sized diamond grains along with *n-D* and *i-C* clusters, which were surrounded by *a-C* grain boundaries. Due to low resistivity, high refractive index, and transmittance, the NDD films headed its attraction to energy conversion or bio-sensing fields.

This work was supported by the Polish National Science Centre (NCN) under Grant Nos. 2014/14/M/ST5/00715 and 2015/17/D/ST5/02571. The DS funds of the Faculty of Electronics, Telecommunications, and Informatics and the Faculty of Chemistry at the Gdansk University of Technology are also acknowledged. Kamatchi J. Sankaran is an FWO Postdoctoral Fellow of the Research Foundations—Flanders (FWO). R. Bogdanowicz wants to thank Prof. W. A. Goddard for invitation and hosting in California Institute of Technology. The Fulbright Commission is acknowledged for financial support of this fellowship.

[1]K. Subramanian, W. P. Kang, J. L. Davidson, N. Ghosh, and K. F. Galloway, Microelectron. Eng. **88**, 2924 (2011).
[2]G. Davies, *Properties and Growth of Diamond* (INSPEC, the Institution of Electrical Engineers, 1994).
[3]M. Umeno and S. Adhikary, Diamond Relat. Mater. **14**, 1973 (2005).
[4]M. Ficek, R. Bogdanowicz, and J. Ryl, Acta Phys. Pol., A **127**, 868 (2015).
[5]R. Bogdanowicz, M. Sobaszek, J. Ryl, M. Gnyba, M. Ficek, Ł. Gołuński, W. J. Bock, M. Śmietana, and K. Darowicki, Diamond Relat. Mater. **55**, 52 (2015).
[6]V. S. Vavilov, Phys. Status Solidi A **31**, 11 (1975).
[7]K. Okano, H. Naruki, Y. Akiba, T. Kurosu, M. Iida, and Y. Hirose, Jpn. J. Appl. Phys. **27**, L173 (1988).
[8]P. Wurzinger, P. Pongratz, P. Hartmann, R. Haubner, and B. Lux, Diamond Relat. Mater. **6**, 763 (1997).
[9]K. J. Sankaran, N. H. Tai, and I. N. Lin, J. Appl. Phys. **117**, 075303 (2015).
[10]S. R. P. Silva, J. Robertson, G. a. J. Amaratunga, B. Rafferty, L. M. Brown, J. Schwan, D. F. Franceschini, and G. Mariotto, J. Appl. Phys. **81**, 2626 (1997).
[11]A. Badzian, T. Badzian, and S.-T. Lee, Appl. Phys. Lett. **62**, 3432 (1993).
[12]Y. Hayashi, G. Yu, M. M. Rahman, K. M. Krishna, T. Soga, T. Jimbo, and M. Umeno, J. Appl. Phys. **89**, 7924 (2001).
[13]K. Panda, B. Sundaravel, B. K. Panigrahi, P. Magudapathy, D. N. Krishna, K. G. M. Nair, H.-C. Chen, and I.-N. Lin, J. Appl. Phys. **110**, 044304 (2011).
[14]S. Bohr, R. Haubner, and B. Lux, Appl. Phys. Lett. **68**, 1075 (1996).
[15]A. C. Ferrari, B. Kleinsorge, N. A. Morrison, A. Hart, V. Stolojan, and J. Robertson, J. Appl. Phys. **85**, 7191 (1999).
[16]L. K. Cheah, X. Shi, J. R. Shi, E. J. Liu, and S. R. P. Silva, J. Non-Cryst. Solids **242**, 40 (1998).
[17]S.-G. Lim, S. Kriventsov, T. N. Jackson, J. H. Haeni, D. G. Schlom, A. M. Balbashov, R. Uecker, P. Reiche, J. L. Freeouf, and G. Lucovsky, J. Appl. Phys. **91**, 4500 (2002).
[18]J. A. Bennett, J. Wang, Y. Show, and G. M. Swain, J. Electrochem. Soc. **151**, E306 (2004).
[19]Y. Tanaka, M. Furuta, K. Kuriyama, R. Kuwabara, Y. Katsuki, T. Kondo, A. Fujishima, and K. Honda, Electrochim. Acta **56**, 1172 (2011).
[20]See supplementary material at http://dx.doi.org/10.1063/1.4953779 containing detailed XPS, Raman studies and HR TEM images.
[21]A. T. Sowers, B. L. Ward, S. L. English, and R. J. Nemanich, J. Appl. Phys. **86**, 3973 (1999).
[22]D. S. Dandy, Thin Solid Films **381**, 1 (2001).
[23]R. Bogdanowicz, M. Sawczak, P. Niedzialkowski, P. Zieba, B. Finke, J. Ryl, J. Karczewski, and T. Ossowski, J. Phys. Chem. C **118**, 8014 (2014).
[24]J. Ryl, R. Bogdanowicz, P. Slepski, M. Sobaszek, and K. Darowicki, J. Electrochem. Soc. **161**, H359 (2014).
[25]J. Ryl, L. Burczyk, R. Bogdanowicz, M. Sobaszek, and K. Darowicki, Carbon **96**, 1093 (2016).
[26]P. Kovarik, E. B. D. Bourdon, and R. H. Prince, Phys. Rev. B **48**, 12123 (1993).
[27]S. Prawer, J. L. Peng, J. O. Orwa, J. C. McCallum, D. N. Jamieson, and L. A. Bursill, Phys. Rev. B **62**, R16360 (2000).
[28]H. Hirai and K.-I. Kondo, Science **253**, 772 (1991).
[29]E. D. Palik, *Handbook of Optical Constants of Solids*, 1st ed. (Academic Press, Boston, 1991), Vol. 2.
[30]M. Gioti, D. Papadimitriou, and S. Logothetidis, Diamond Relat. Mater. **9**, 741 (2000).
[31]*Handbook of Ellipsometry*, 1st ed. edited by H. G. Tompkins and E. A. Irene (William Andrew, Norwich, NY, Heidelberg, Germany, 2006).
[32]H. Kinoshita, T. Hando, and M. Yoshida, J. Appl. Phys. **89**, 2737 (2001).
[33]A. Gharibyan, D. Hayrapetyan, Z. Panosyan, and Y. Yengibaryan, Appl. Opt. **50**, G69 (2011).
[34]S. Jin and T. D. Moustakas, Appl. Phys. Lett. **65**, 403 (1994).
[35]J. Robertson, Mater. Sci. Eng., R **37**, 129 (2002).